

# Effect of Tellurium Substitution on the Properties of Iron Di-Selenide

D.K. Sharma<sup>1</sup>, Bhavna Joshi<sup>2</sup>, K. R. Patel<sup>2</sup>, V.Ganeshan<sup>3</sup>, Y. K. Sharma<sup>1</sup>

<sup>1</sup>Physics Department, University of Rajasthan, Jaipur (Rajasthan), India

<sup>2</sup>Physics Department, J. N. V. University, Jodhpur (Rajasthan), India.

<sup>3</sup>Physics Department, UGC, DAE CSIR Indore (M.P.), India.

Email: dksharma.phy@gmail.com

**Abstract-** FeSe<sub>2</sub> and FeTe<sub>2</sub> both crystallize in C-18 Marcasite type orthorhombic structure. We have attempted to substitute tellurium in FeSe<sub>2</sub> by solid state reaction method and polycrystalline samples Fe(Se<sub>2-x</sub>Te<sub>x</sub>) with x=0.2,0.6,1.0,1.4,1.8 were synthesis to study the effect of substituting Te with Se in FeSe<sub>2</sub>. Phillips X-ray diffractometer is recorded XRD patterned using CuK<sub>α</sub> radiation into 2θ range of 10<sup>0</sup> to 90<sup>0</sup>. XRD revealed that both the samples posses orthorhombic The lattice parameter and the cell volume increases monotonically with increasing Te concentration structure Scanning electron microscopy (SEM) reveals irregularly shaped particle with an average size 254.5nm to 678.2nm. <sup>57</sup>Fe Mossbauer spectroscopy experiments were performed at 300K using <sup>57</sup>Co Rhodium source. Mossbauer spectra of Fe(Se<sub>2-x</sub>Te<sub>x</sub>) with x=0.2,0.6,0.8,1.0,1.4 & 1.8 revealed paramagnetic character Isomer shift(IS)and qudropole shift (QS) vary considerably with absence of internal hyperfine fields compared to pure FeSe<sub>2</sub>. Electrical resistivity of Fe(Se<sub>2-x</sub>Te<sub>x</sub>) with x=0.6 and 1.0 revealed that the samples shows semiconducting behavior in case of variation of resistance with magnetic field at different temperatures.

**Keywords-** X- ray diffraction, Mossbauer effect, Scanning electron microscopy, Electrical resistivity.

## I INTRODUCTION

The crystal structures of the marcasite modification of FeSe<sub>2</sub>, FeTe<sub>2</sub> (the mineral marcasite) have been determined at room temperature from three dimensional single crystal X ray data. Using the Hamilton test in the judgment between the number of possible model for each structure, the space group was found to be Pnn2. Compared with the symmetry hitherto assumed for the FeS<sub>2-m</sub> type, these structures lack the mirror plane

perpendicular to (001) at z = 1/2( and z = 0).The unit cell contains 2T in position(a) with z=0 and 4X in position (c) with x=0.2241(1), y=0.3620(1), z=0.0218(28) for FeTe<sub>2</sub> (Standard deviation are appended in brackets. FeS<sub>2-m</sub> show anisotropic thermal motion in the three structures. FeSe<sub>2</sub> FeTe<sub>2</sub> are to be assumed the stoichiometric 1:2 composition without having any appreciable range of homogeneity, whereas the FeTe<sub>2</sub> phase exhibit homogeneity range from 66.6±0.2 to 67.4±0.2 atomic percent Te at 450(8) °A, c=3.8738(7) °A for FeTe<sub>2</sub> has been obtained from stoichiometric composition as average value for several independent samples [1].

Mossbauer spectra FeTe<sub>2</sub> at 4.2K, it can be seen that chemical shifts (δ) and total line width of these spectra are equal within experimental error, although their maximum absorption effects differ. There are no resolved qudropole or magnetic hyperfine interaction observed for any of the compound. However, the peaks appears to be true broad to be accounted for by single lines and consequently they were computer fitted assuming qudropole split lines of equal width and intensity .δ=-0.03mm/s, Δ=3.32mm/s and ,line-width Γ=12.46mm/s. The qudropole coupling which is present in FeTe<sub>2</sub>, as a consequence of the distortion from T<sub>d</sub> symmetry of the coordination polyhedral around Te, is only resolved by restoring to computer fitting a measure of angular part of the distortion from cubic symmetry is given by the average deviation of the bond angles from the tetrahydal values of 109.5<sup>0</sup>, the average deviation for FeTe<sub>2</sub> is 10.1<sup>0</sup> [2].

Extensive studies have been done on the transition metal (M) mono chalcogenides and dichalcogenides, because of their interesting electrical and magnetic properties in great varieties ranging from insulating to metallic and from paramagnetic to ferromagnetic (anti ferromagnetic) in the series of the compounds. These studies have been done from a point of view of Mott-Hubbard model, where the band gap is formed from the onsite d-d Coulomb interaction energy  $U$  dominating over the d band dispersion. Recently, Zaanen and Sawatzky [3], Bocquet et al. [4] and Fugimori et al. [5] have revealed the general trend of electronic structure of M compounds a cluster type configuration interaction analysis of the photoemission spectra of M monoxides, chalcogenides. They have shown that the band gap of the insulating compound of the late transition metals are of the charged transfer type characterized by a ligand-to-metal charge transfer energy  $\Delta$  and that the gap of the early transition matter compounds of a Mott-Hubbard model.

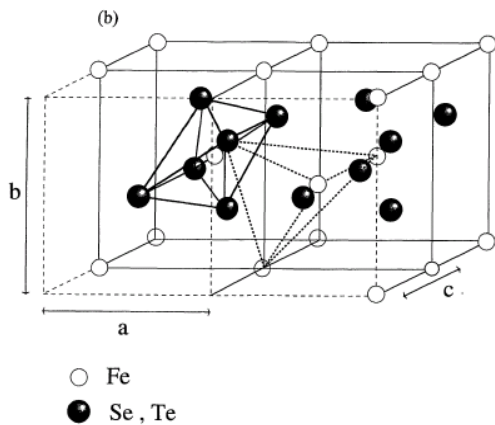


Fig.1 Marcasite type  $\text{FeSe}_2$  &  $\text{FeTe}_2$  orthorhombic structure

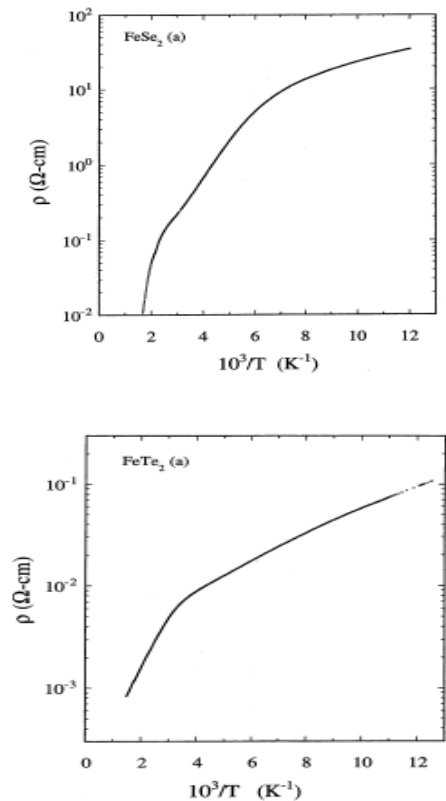


Fig.2.  $\text{FeSe}_2$  and  $\text{FeTe}_2$  are semiconductor having energy gap  $E_g$  of about 1eV and 0.46eV respectively

It is known that iron dichalcogenides  $\text{FeX}_2$  ( $X=\text{S}, \text{Se}$  and  $\text{Te}$ ) are semiconducting compound [6-7] arite type crystal structure [8] and both  $\text{FeSe}_2$  and  $\text{FeTe}_2$  the marcasite of the calculated qudrpole splitting as shown fig.2. Electrical resistivity is the important electric transport property because to get essential information about the electronic state of these semiconductor compounds. Electrical resistivity for  $\text{FeSe}_2$  was measured on sintered poly crystals by fisher [9] and by Dudkin and Baidanich [10]. The qudrpole splitting of  $^{57}\text{Fe}$  in  $\text{FeSe}_2$  the marcasite structure is shown to correlate well with electric field gradient at the Fe site, calculated on the point charged model derivation these compounds are in the direction to be expected from covalent effects and from the distortion of the local environment of the iron atoms. The change of crystal structure from  $\text{FeS}_2$  (P) to  $\text{FeSe}_2$ (M) decreases the

octahedral symmetry of iron metals(NN) surroundings and should thus be expected to increase  $\Delta E_Q$  ( $0.584 \pm 0.010$  mm/s at 300 K) [11]. The Mössbauer parameter and their variation with temperature were accounted for by the reasonable value of the parameters.  $^{57}\text{Fe}$  Mössbauer studies at 300K had been carried out by Y.K. Sharma et.al. [12] concluded marcasite–arsenopyrite–marcasite type structural transition on the basis of quadrupole splitting variation with tellurium substitution for antimony into  $\text{FeSe}_{2-x}\text{Te}_x$  system. This result is in conformity with the earlier finding by Yamaguchi et.al. [13] that the compositions between  $\text{FeSe}_{1.6}\text{Te}_{0.6}$  and  $\text{FeSe}_{0.6}\text{Te}_{1.4}$  are arsenopyrite type pseudo–orthorhombic or monoclinic whereas all other compositions towards the end members are marcasite type orthorhombic structure. We therefore aim to synthesize pseudo binary  $\text{FeSe}_{2-x}\text{Te}_x$  for finding out the changes in various physical properties such as structural, electrical, electronic and magnetic properties. We present here briefly the studies done using powder XRD and Mössbauer Spectroscopic techniques. We therefore here describe our efforts to synthesize and characterize anionically substituted  $\text{FeSe}_2$  systems viz. with 3.33 atom % Te substitution for Se into  $\text{FeSe}_2$ . In this work, we report first time the synthesis, X-ray diffractometer (XRD), Scanning Electron Microscopic (SEM), Mössbauer  $^{57}\text{Fe}$  iron studies at 300K as well as the electrical properties of  $\text{FeSe}_{2-x}\text{Te}_x$  ( $x=0.4, 0.8, 1.0, 1.2$  &  $1.6$ ).

## II EXPERIMENTAL METHODS

Polycrystalline samples of  $\text{Fe}(\text{Se}_{2-x}\text{Te}_x)$  with  $x=0.2, 0.6, 1.0, 1.4, 1.8$  were synthesized from Fe (Baker 99.99%) Se (Alfa Aesar 99.5%) and Te (Alfa Aesar 99.999%) mixed in stoichiometric amounts, sealed in an evacuated quartz tube and heated at  $1000^\circ\text{C}$  for 7 days, after which they were cooled to the room temperature and annealed at  $580^\circ\text{C}$  for next 14 days and quenched at  $580^\circ\text{C}$  in cold water. The resulting samples were ground to obtain the fine powders to perform the measurements mentioned above. Phased identification

of the powdered sample was performed with a Siemens D5000 X-ray diffractometer using  $\text{Cu-K}\alpha$  radiation and a Ni filter. Intensities were measured at room temperature in  $0.02^\circ$  steps, in the  $10^\circ$ - $90^\circ$   $2\theta$  range. The crystallography phases  $2\theta$  ranges. The crystalline phases were identified by comparison with the X-ray pattern of the JCPDS database. In order to perform the analysis, the spectra were refined using the Rietica Rietveld program,  $v$  1.71 with multiphase capability. Thin absorber were made with powder of the samples to record at room temperature Mossbauer spectra in a transmission with a geometry a constant oscillation spectrometer using a  $^{57}\text{Co}$  Mossbauer source in a Rhodium matrix. All the spectra were fitted using the Recoil 1.05 [14] program and the isomer shifts are quoted with respect  $\text{Fe}_a$  to ion. Electrical resistivity in presence of magnetic field and its variation with temperature measure using four probe methods.

## III EXPERIMENTAL DETAILS

Polycrystalline samples of Te doped  $\text{FeSe}_2$  were prepared using the conventional solid-state reaction method. Stoichiometric  $\text{FeSe}_{1.6}\text{Te}_{0.4}$  and  $\text{FeSe}_{1.2}\text{Te}_{0.8}$  were weighed and kept in sealed quartz ampoules ( $10^{-2}$  Torr) and treated at  $1073\text{K}$  for 10 days and annealed at  $853\text{K}$  for another 10 days and quenched  $853\text{K}$ . The phase and the crystallographic structure of the samples were determined by XRD using a Philips make X'Pert X-ray diffractometer equipped with  $\text{Cu K}\alpha$  radiation. The XRD patterns were recorded in the  $2\theta$  range of  $10^\circ$ - $90^\circ$  with a step size of  $0.020^\circ$ .  $^{57}\text{Fe}$  Mössbauer experiments were performed at  $300\text{K}$  using  $^{57}\text{Co}$  (Rh) source in constant acceleration mode and calibrated using natural iron.  $^{57}\text{Fe}$  Mössbauer measurements at  $300\text{K}$  were performed using a  $10\text{ mCi } ^{57}\text{Co}$  (Rh) source moving in constant acceleration mode. The data were collected on to an MCD / PC using 512 channels. The Mössbauer spectra corresponding to the alloy specimens were calibrated using natural iron foil. The absorbers were prepared typically using  $4\text{ mg/cm}^2$  of natural iron content for these specimens which corresponds to 50

mg/cm<sup>2</sup> of the specimen. The relative absorption in Mössbauer spectra observed varied from 4.42 % to 6.80 % for these specimens. The absorber (sample) was sandwiched in between two aluminium foils to achieve a good thermal equilibrium. The Mössbauer spectra of all specimens were fitted using a standard data analysis program.

#### IV RESULTS AND DISCUSSION

##### A) X-Ray Diffraction Analysis

Fig. 3 shows the XRD patterns for all five specimens, which were indexed and analyzed using “Powder X” indexing program [4]. The experimental peaks, and (hkl) indexing, have been shown in this figure. For all the series specimens, the large intensity peaks observed corresponds to the reflections (011), (111), (211), (031) and (122). Table I displays the indexed peaks, experimental and calculated 2 $\theta$  and their differences, experimental and calculated d values and the intensities of the indexed and unindexed reflections found through “Powder X” indexing program [4]. The asterisked peaks correspond to CuK $\alpha$  radiation. There is neither any intense peak corresponding to an elemental impurity of Fe or Se or other elements like Te, or their binary phases e.g. FeSe<sub>2</sub>, etc. observed in the patterns of the series specimens. Table I shows the lattice parameters (a, b, c) and unit cell volume (V) for all four compositions. It displays the lattice parameters (a, b, c) and unit cell volume (V) plotted against the atomic number of substituted anions. It reveals the increase in the lattice parameters and unit cell volume upon anionic substitution of elements from Se to Te. There is a variation of 2 % in unit cell volume on substitution for Te in FeSe<sub>2</sub>. The lattice parameters for FeSe<sub>2</sub> match well with those reported earlier by Petrovic et.al. [15]. The unit cell volume for FeSe<sub>1.8</sub>Te<sub>0.2</sub>, FeSe<sub>1.6</sub>Te<sub>0.4</sub>, FeSe<sub>1.0</sub>Te<sub>0.1</sub>, FeSe<sub>0.8</sub>Te<sub>1.2</sub> and FeSe<sub>0.4</sub>Te<sub>1.6</sub> less than FeSe<sub>2</sub>. These results may be attributed to the increasing substituent atom size (of the anionic atom) as one goes from Te from 0.4 to 1.4. The observed XRD patterns of

first major three Bragg peaks in the observed diffractograms of Fe(Se<sub>2-x</sub>Te<sub>x</sub>) with x=0.2,0.6,1.0,1.4&1.8 matches well with the simulated diffraction patterns. Preliminary analysis of XRD patterns indicate that both the samples crystallize in marcasite type orthorhombic structure (JCPDS No.21-0432) belonging to the space group *Pnmm* (No.58). The obtained values of the lattice parameters listed on the XRD patterns clearly indicate that introduction of Te for Se in FeSe<sub>2</sub> leads to monotonic enhancement in the unit cell volume increased from 103.98 m<sup>3</sup> to 128.43m<sup>3</sup> with Te concentration. To study this and other possible structural changes X-ray diffraction studies were made, including Rietveld analysis of the x-ray patterns in Fig.4 for FeSe<sub>2</sub> and FeTe<sub>2</sub>.

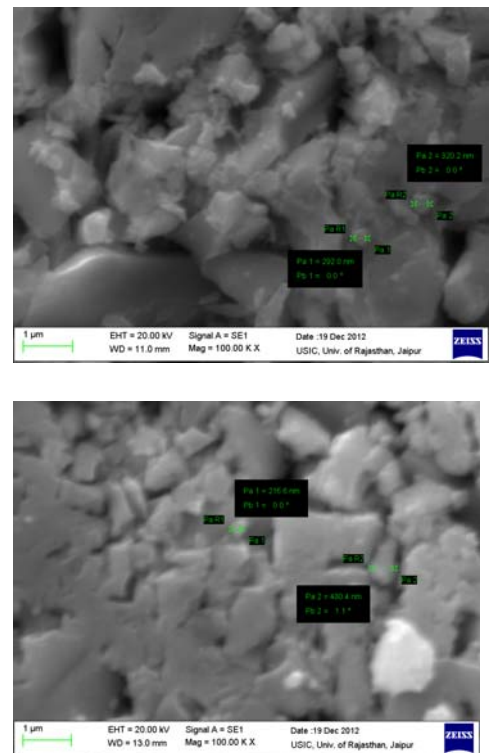


Fig.5. SEM images of Fe(Se<sub>2-x</sub>Te<sub>x</sub>) with x=0.2&1.8

### B. SEM images of $Fe(Se_{1-x}Te_x)_2$ with $x=0.2$ & $1.8$

SEM images of  $Fe(Se_{1-x}Te_x)_2$  indicated that the size of the particle Pa R1 is smaller than Pa R2 in  $FeSe_{1.8}Te_{0.2}$  and  $FeSe_{0.2}Te_{1.8}$  samples in fig.(5). In  $FeSe_{1.8}Te_{0.2}$  the size of particles for Pa R1 (Pa1=292.0nm ; Pb 1=0.00) and the comparatively size another particle Pa R2(Pa 2=320.20 nm; Pb=0.00) this reveals that size of Pa R2 is greater than Pa R1. In  $FeSe_{0.2}Te_{1.8}$  the size of particles for Pa R1(Pa 1=216.6nm ; Pb 1=0.00) and the comparatively size another particle Pa R2 (Pa 2=480.9nm; Pb=1.10) this shows that size of Pa R2 is greater than Pa R1.

### C. $^{57}Fe$ Mössbauer Measurements

#### Spectra at 300K

Fig.3 shows the  $^{57}Fe$  Mössbauer spectra at 300K for the specimens  $FeSe_{1.8}Te_{0.2}$ ,  $FeSe_{1.6}Te_{0.4}$ ,  $FeSe_{1.0}Te_{0.1}$ ,  $FeSe_{0.6}Te_{1.4}$  and  $FeSe_{0.2}Te_{1.8}$  respectively. The experimental data points have been shown by dots where as the solid line is the computed envelope of the single quadrupole split. Table II gives the values of Mössbauer parameters viz. Isomer shift (IS), Quadrupole splitting (QS), Line width (LW) and  $\chi^2$ , the goodness-of-fit parameter. Each spectrum was fitted with an acceptable  $\chi^2$ . The line width of the specimens ranges between 0.4328 mm/s to 0.2566 mm/s, which is comparable with the width for standard natural iron absorber at 300K. The  $^{57}Fe$  Mössbauer spectra for all specimens therefore indicate paramagnetic character at 300K.

#### Isomer Shift (IS)

It may be seen from Table II that IS values do not exhibit much change from Te substitution for Se into  $FeSe_2$  and are indicative of iron staying in the low spin state with highly covalent Fe-Se(X) bonds in all these compositions as in the case of  $FeSe_2$ . This fact is in accordance with the earlier findings of Temperley et al. [16]. The constancy of isomer shift around the value

0.4782 mm/s to 0.3962 mm/s (with respect to iron metal) for these series compositions may be explained qualitatively as follows: The isomer shift is mainly measure of s-electron density at the nucleus of the Mössbauer atom (Fe atom at present). This s-electron density is mainly contributed from two factors; one is from filled s-orbitals in inner electron shells and another from partially filled outer most orbitals (valence orbitals) where the Mössbauer atom's own valence electrons as well as electrons from surrounding ligands are accommodated constituting the chemical bond. This valence electron contribution is very much sensitive to changes in electronic configuration of valence shell. This valence electron population is subject to change by substituting the chalcogen atom (e.g. S, Se, Te) or a pnictogen atom (e.g. P, As etc.) for antimony as it will be replaced in the iron octahedral surrounding in the first coordination sphere and due to electronegativity difference it will also affect Se-Fe-X type covalent bonds. It has been shown that the order of increasing electro negativity of the ligands is  $S < As < Se < Te$  (Pauling 1960 [17]) which has clearly been exhibited by the increasing IS values for the compounds  $FeS_2$ ,  $FeSe_2$  and  $FeTe_2$  all orthorhombic structured marcasites similar to the ones we have synthesized by substituting S or Sb or Te or As for Se into  $FeSe_2$ . However, since we have substituted only 3.33 atom% of these chalcogen or pnictogen atom, the number of Se-Fe-X bonds compared to Se-Fe-Se bonds will not be significant and hence one may expect the constancy of IS values. We would like to add that due to low spin state as well there may not be a significant change in IS values while substituting the anions as also was observed by Y.K. Sharma et al. [18] for  $Fe(Sb_{1-x}Te_x)_2$  series compositions through  $^{57}Fe$  Mössbauer studies at 300 K.

#### Quadrupole splitting (QS)

The QS values exhibit a small increase in (Table II) going from 0.2 to 1.8 Te substituted  $FeSe_2$  compositions of the series. One may understand this change in QS as: The QS is a measure of the asymmetry of the total

electronic wave function (or EFG) at the Fe nucleus which could be due to two factors. One of these is from the valence electron contribution and the other from the lattice. Due to increase in unit cell volume of about 2 %, on going from 0.2 to 1.8 Te substitutions for Sb, the lattice contribution to the QS may also be expected to increase. As anionic substitution may be expected to affect the covalent character of Se-Fe-X type bonding which in turn will affect the degree of distortion of the iron octahedral coordination [19]. This should increase the lattice contribution to the QS. Hence, the net QS value may increase on going from Te substitution for Se for the series specimens.

### Anion distribution and site population

It is worthwhile to know how the substituted anion is distributed among the lattice sites. One may understand the nature of site assignments for the doublets by assuming a statistically random distribution of the anions studied in the series. This kind of distribution has been successfully applied by several workers for understanding the variation of quadrupole splitting for different solid solutions [20-23]. Under this distribution, if in the present series Z is taken as the number of anions (S, As, Se and Te) in a system so that (2-Z) becomes the number of Se ions, then different terms in the expansion represent the probabilities of the occurrence of different kinds of environments around Fe atoms having octahedral configuration where the first term is proportional to the probability of occurrence of 6Se ions in the first coordination sphere of Fe, the second to the (5Sb, 1X) anions, the third to (4Sb, 2X) anions and so on [24]. Using this equation, the normalized percentage probabilities for all seven possibilities [(6Se, 0X), (5Se, 1X), (4Se, 2X), (3Se, 3X), (2Se, 4X), (1Se, 5X) and (0Se, 6X)] for each composition [25].

The results are given in Table II. Using these probabilities, one may find theoretically the doublet area ratio (or site population ratio) assuming a particular grouping of different kinds of Fe octahedra. One finds

that if one attributes all octahedra with  $\geq 5$ Se anions to first quadrupole doublet (say site A) and all those with  $< 5$ Se anions to the second quadrupole doublet (site B), then the area ratio (B/A) predicted using the binomial expansion for anionic distribution in iron octahedra is less than 4%. It is clear from this theoretical exercise that the doublet area of weaker site is too less to be resolvable in the experimental spectra. Due to this weaker and unresolvable second quadrupole doublet (say site B) we fitted single quadrupole doublet for all five specimens of the series.

### D. Electrical Properties

In case of sample (S1) FeSeTe the variation of resistance with magnetic field at different temperature (2K, 25K, 50K, 100K, 200K, 250K and 300K) are measured. From the observation it is clear that resistance almost remains constant with the magnetic field from 0 to 140000 Oe. At temperature 2K comparatively larger increase in resistance with field. The resistance rises by seven times at temperature 2K as compare to room temperature. In case of sample (S2) FeSe<sub>0.4</sub>Te<sub>1.6</sub> the variation of resistance with magnetic field at different temperature (2K, 25K, 50K, 100K, 200K, 250K and 300K) are measured. From the observation it is clear that resistance almost remains constant with the magnetic field from 0 to 140000 Oe. At temperature 2K comparatively larger increase in resistance with field. The resistance rises by 1.5 times at temperature 2K as compare to room temperature. As concentration of tellurium is increased variation in ratio of resistance at temperature 2K and room temperature is comparatively very small.

The variation magnetoresistance of sample (S1) with temperature at different values of magnetic field (1T, 3T, 5T, 7T, 9T, 12T and 14T) are observed. At low temperature 4K to 50K magnetoresistance decreases rapidly in comparison to 50K to 225K. Further in the temperature of 225K to 300K again magnetoresistance decreased in larger amount. Since

magnetic field is increased from 1T to 14T at low temperature less than 40K magnetoresistance is increased three times (15% to 45%)

The variation magnetoresistance of sample  $\text{FeSe}_{0.4}\text{Te}_{1.6}$  (S2 MR) with temperature at different values of magnetic field (1T, 3T, 5T, 7T, 9T, 12T and 14T) are observed. At low temperature 4K to 50K magnetoresistance decreases rapidly in comparison to 50K to 225K. As the concentration of tellurium is increased rate of loss in magnetoresistance is more at 14T as compare to the less values of magnetic field. Further in the temperature of 225K to 300K again magnetoresistance slightly increased in larger amount. Since magnetic field is increased from 1T to 14T at low temperature less than 40K magnetoresistance is increased four times (2% to 8%). Thus we conclude that as Te increases rate of percentage of magnetoresistance at low temperature is increased. In  $\text{FeSe}_{0.8}\text{Te}_{1.2}$  the electric resistance decreases with temperature exponentially at low temperature and almost linearly at higher temperature 100K to 300K. At zero field resistance almost 14 ohm at 4K which is approximately two-third or 33% less than at 14T at same temperature. For each increase in magnetic field 1T resistance increase by 6% to 8%. Since at 1T resistance is less than as compared to 0T from 4K to 400K but in case of 3T at low temperature below 150K resistance is more than zero field resistance and at 150K both values become equal to 1.7 ohm and above this temperature R decreases in the same pattern. At 300K the resistance is independent of magnetic field. Thus as temperature decrease the resistance is increased with magnetic field above 3T. In  $\text{FeSe}_{0.4}\text{Te}_{1.6}$  the electric resistance decreases with temperature exponentially at low temperature and almost linearly at higher temperature 100K to 300K. At zero field same temperature. For each increase in magnetic field 1T resistance increase by 6% to 8%. Since at 1T resistance is less than as compared to 0T from 4K to 300K but in case of 3T at low temperature below 150K resistance is more than zero field resistance and at 150K both values become resistance almost 0.058 ohm at 4K

which is approximately two-tenth or 2 % less than at 14T at equal to 0.050 ohm and above this temperature R decreases in the same pattern. At 300K the resistance is independent of magnetic field. Thus as temperature decrease the resistance is increased with magnetic field above 3T. Conclusion Te can be substituted in  $\text{FeSe}_2$  in C-18 type orthorhombic structure up to  $x=0.8$ . Mössbauer Spectra reveal that both of these compositions are not magnetically ordered at 300K and IS and QS varies considerably compared to  $\text{FeSe}_2$ .

## V CONCLUSIONS

On the basis of the experimental data we conclude that

- The XRD analysis suggests the single phase orthorhombic crystal structure at 300K for and therefore here exist solid solubility of Te into  $\text{Fe}(\text{Se}_{2-x}\text{Te}_x)$  with  $x=0.2, 0.6, 1.0, 1.4, 1.8$  these atoms. The lattice parameters and unit cell volume increases from Te substitution.
- SEM images of  $\text{Fe}(\text{Se}_{2-x}\text{Te}_x)$  indicated that the size of the particle Pa R1 is smaller than Pa R2 in  $\text{FeSe}_{1.8}\text{Te}_{0.2}$  and  $\text{FeSe}_{0.2}\text{Te}_{1.8}$  samples
- $^{57}\text{Fe}$  Mössbauer spectra for all specimens indicate the paramagnetic character at 300K
- The predictions on relative site populations using a binomial expansion for the random distribution of the anions Se and Te in iron octahedra have been made assuming a particular site assignment shows that there exists a stronger site (~ 95% populated) and a weaker site (less populated ~ 3.7%) and hence, Mössbauer parameters of stronger site only have been given in Table II.
- $\text{FeSe}_2$  and  $\text{FeTe}_2$  are semiconductor having energy gap  $E_g$  of about 1eV and 0.46eV respectively
- In case of sample (S1)  $\text{FeSeTe}$  At temperature 2K comparatively larger increase in resistance with field. The resistance rises by 1.5 times at temperature 2K as compare to room temperature. As concentration of tellurium is increased variation in ratio of resistance at temperature 2K and room temperature is comparatively very small.

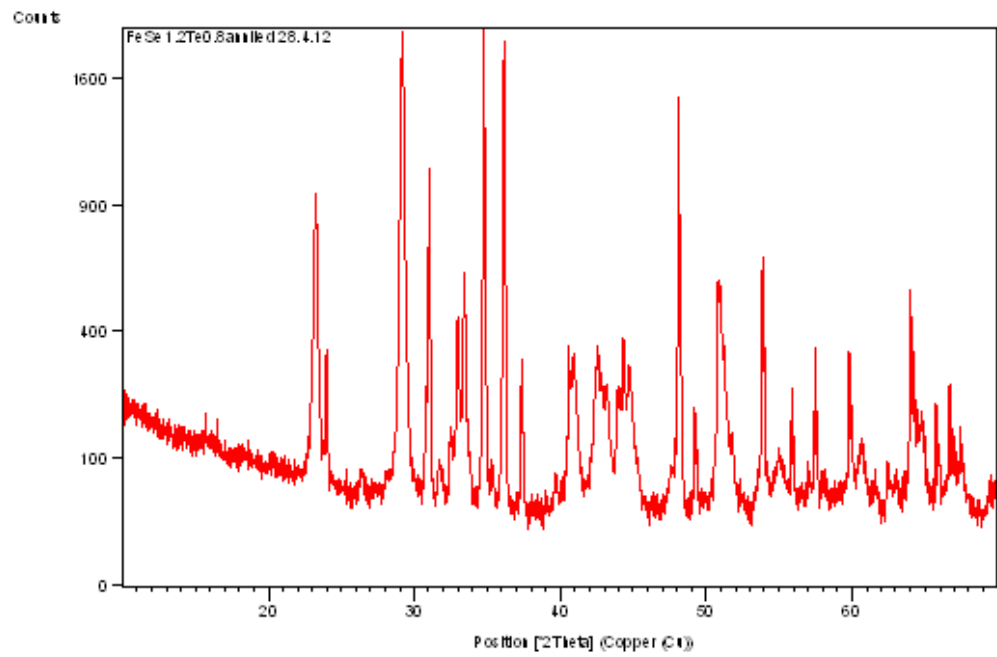
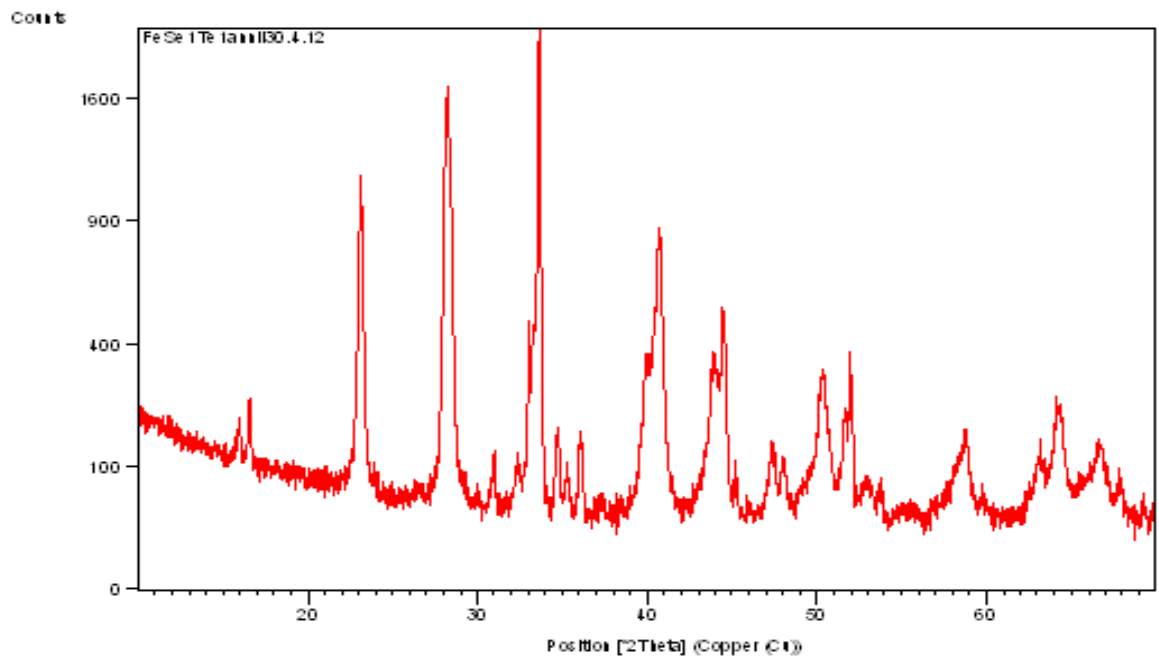
- In  $\text{FeSe}_{0.4}\text{Te}_{1.6}$  the electric resistance decreases with temperature exponentially at low temperature and almost linearly at higher temperature 100K to 300K. At zero field resistance almost 0.058 ohm at 4K which is approximately two-tenth or 2 % less than at 14T at same temperature.

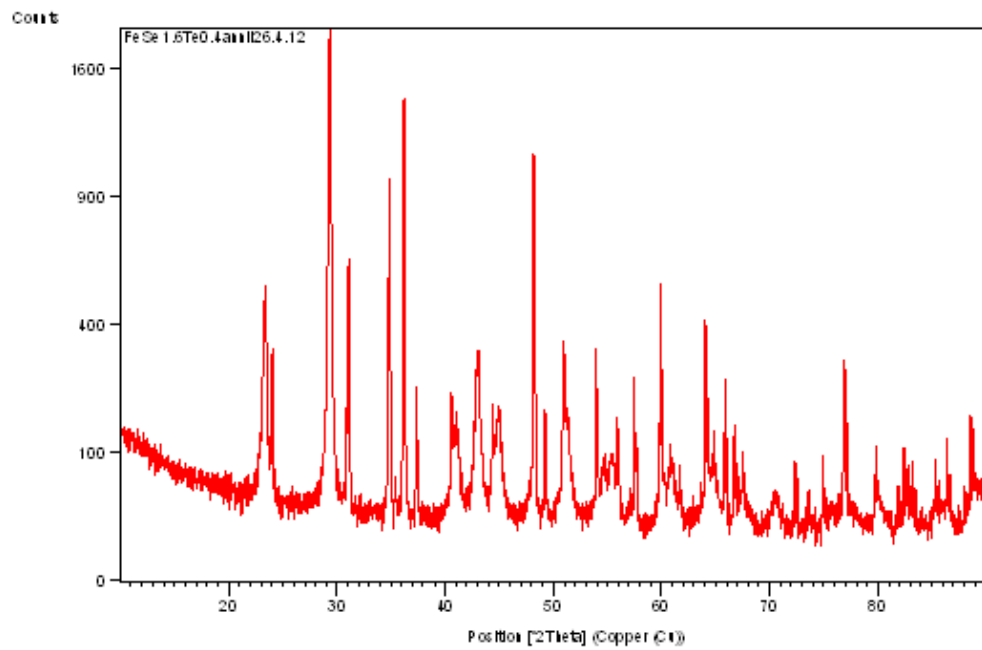
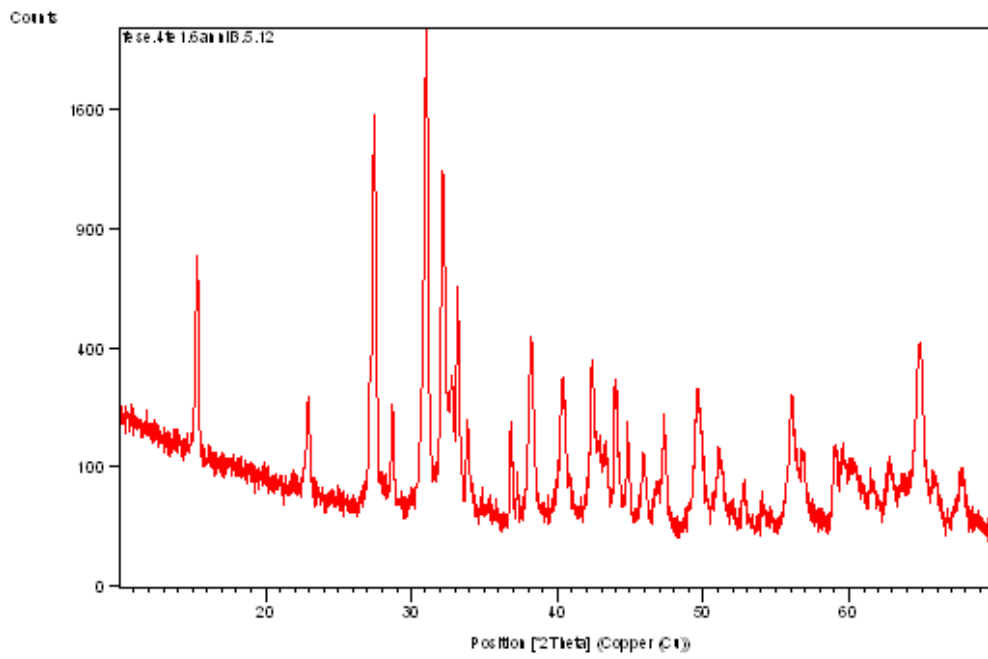
## VI ACKNOWLEDGMENTS

The authors thank UGC DAE CSIR Indore (INDIA), Professor V.Ganesan for resistivity measurement and Dr. Sher Singh (BARC, Mumbai) for Mossbauer analysis. We are thankful to Professor B.K. Shrivastava for Providing XRD measurement facility and SEM measurement for suggesting the marcasite problem.

## VII REFERENCES

- [1] Gunnar Brostigen and Arne Kjekshus Acta Chemica Scandinavica 24 (1970).
- [2] A.Kjekshus and D G Nicholson, Acta Chemica Scandinavica 26 (1972).
- [3] J. Zaanen and G. A. Sawatzky: J. Solid Chem. 88 (1990).
- [4] A. E. Bocquet, T. Mizokawa, T. Saitoh, H. Namatame and A. Fujimori: Phys. Rev. B 46 (1992) 3771.
- [5] A. Fujimori, A. E. Bocquet, T. Saitoh and T. Mizokawa: J. Electron Spectrosc. Relat. Phenom. 62 (1993) 141.
- [6] F. Hulliger and E. Mooser: J. Phys. Chem. Solids 26 (1964) 429.
- [7] R. W. G. Wyckoff: *Crystal structures* (Interscience Publishers, John Wiley & Sons, New York 1963) Vol. 1, p. 348, p. 356.
- [8] Arne Kjekshus, Trond Rakke and Arne F. Andersen, Acta Chemica A 28 ( 1974)- 1000.
- [9] G. Fischer: Can. J. Phys 36 (1958) 1435.
- [10] L. D. Dudkin and V. I. Vaidanich: Sov. Phys. Solid State 6 (1962) 1384.
- [11] Y.K. Sharma and F.E. Wagner, Hyperfine Interactions, 59, 341 (1990).
- [12] Y.K. Sharma, B.K. Srivastava and S. Loknathan, J. Solid State Phys., 14, 859 (1981).
- [13] G. Yamaguchi, M. Shimada and M. Koizumi, J. Solid State Chem., 34, 241 (1980).
- [14] C. Dong, J. App. Cryst., 32, 838 (1999).
- [15] C. Petrovic, Y. Lee & T. Vogt, et al. Phys. Rev. B 72, 045103 (2005).
- [16] A.A. Temperley and H.W. L  f  vre, J. Phys. Chem. Solids, 27, 85 (1966).
- [17] L. Pauling, "The Nature of Chemical Bond", Oxford and IBH Pub. Co., Calcutta, India (1960).
- [18] Y.K. Sharma and F.E. Wagner, Hyperfine Interactions, 59, 341 (1990),.
- [19] N.N. Greenwood and T.C. Gibb, M  ssbauer Spectroscopy, Chapman and Hall London, P 284 (1971).
- [20] G. Filoti, A. Gelberg, V. Gomolea and M. Rosenberg, Int. Journal of Magnetism, 2, 65 (1972).
- [21] F.E. Fujita, "Topics in Applied Physics – M  ssbauer Spectroscopy" edited by U. Gonser Vol. 5, 201 (1975).
- [22] A. Krishnamurthy, B.K. Srivastava and S. Loknathan, Solid State Comm., 39, 983 (1981).
- [23] S.K. Kulshreshtha and P. Raj, Solid State Comm., 28, 787 (1978).
- [24] J.B. Ward and D.G. Howard, J. Appl. Phys., 47, 388 (1976).
- [25] J. Steger and E. Kos tiner, J. Solid State Chem., 5, 131 (1972).





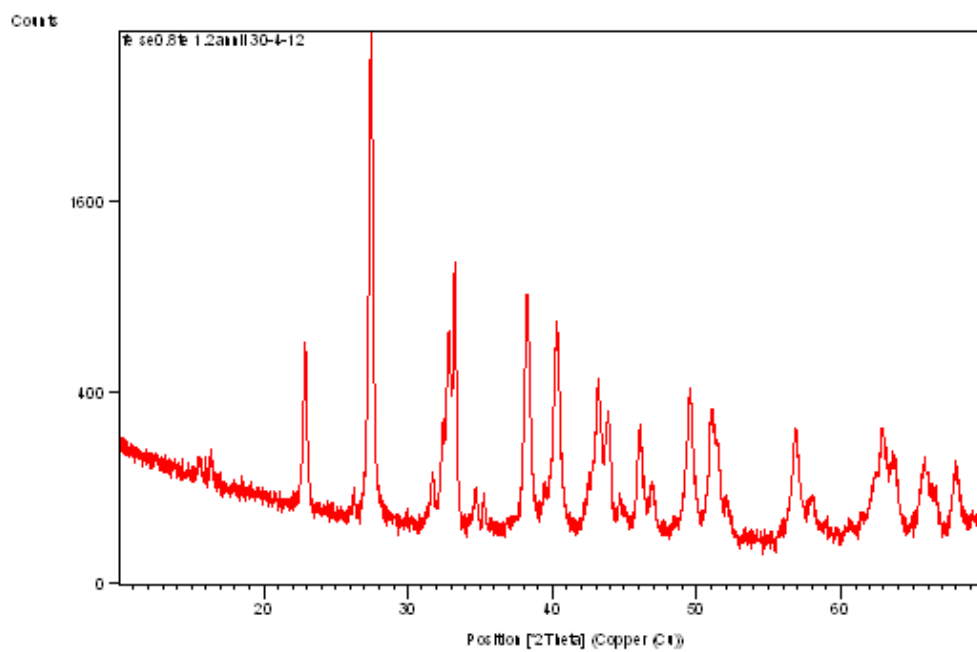
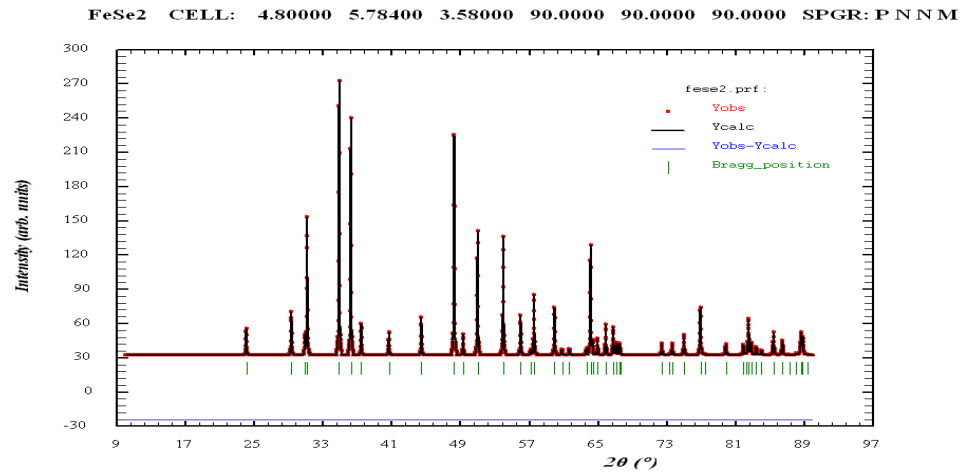
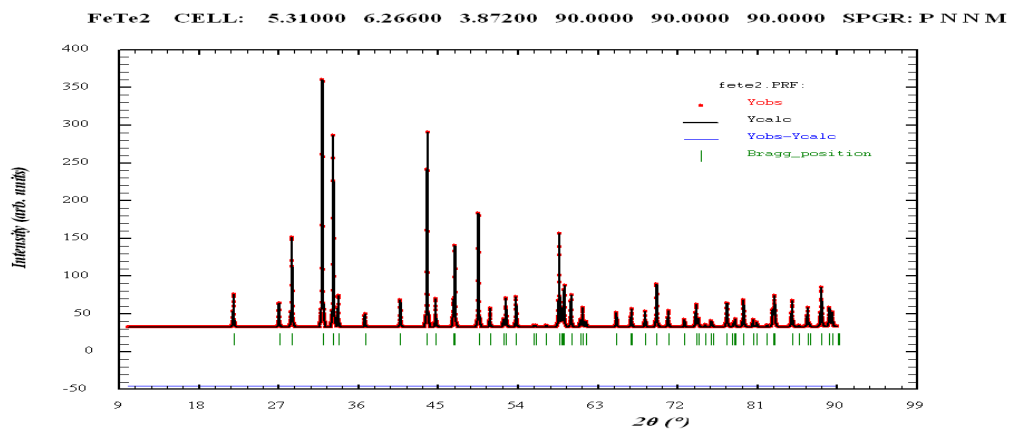


Fig 3. XRD patterns of Fe(Se<sub>2-x</sub>Te<sub>x</sub>) with x= 0.2,0.6,1.0,1.4&1.8

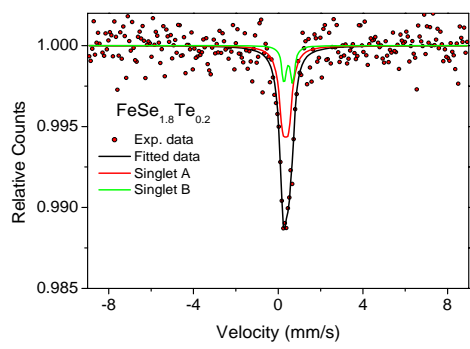


(i)

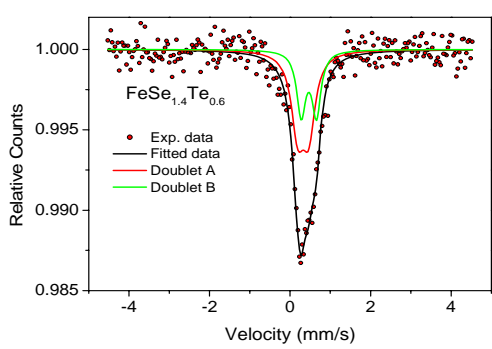


(ii)

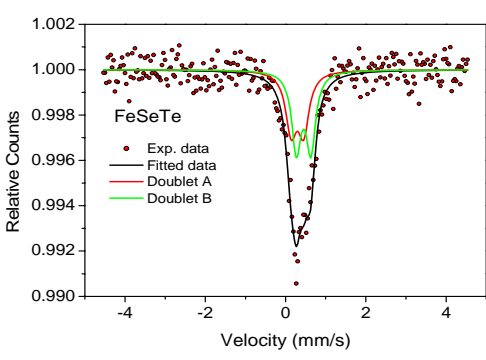
Fig.4. Simulated XRD patterns of (i) FeSe<sub>2</sub> and (ii) FeTe<sub>2</sub>



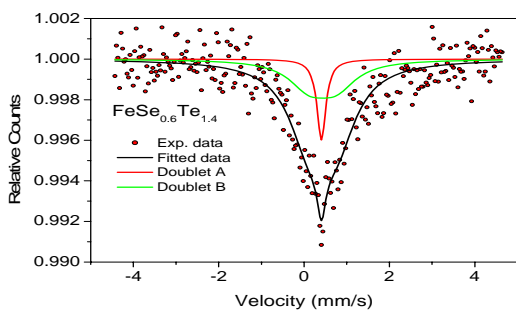
(i)



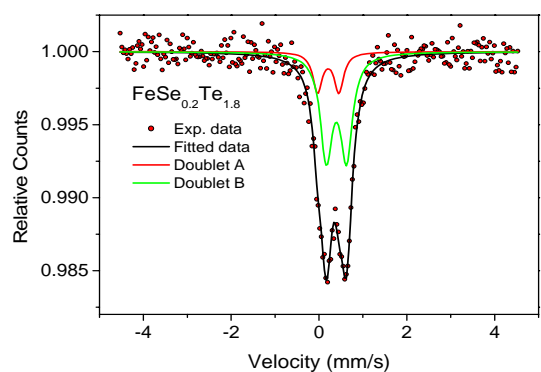
(ii)



(iii)

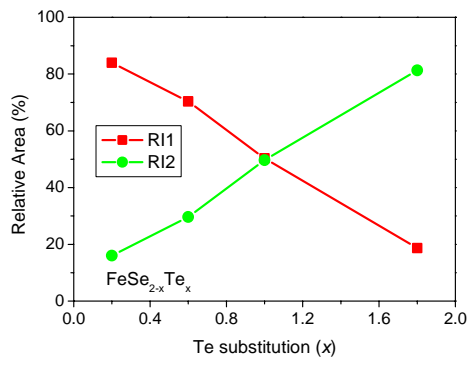


(iv)

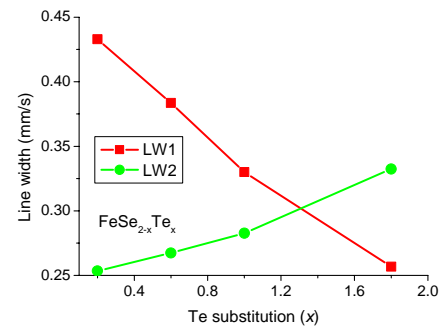


(v)

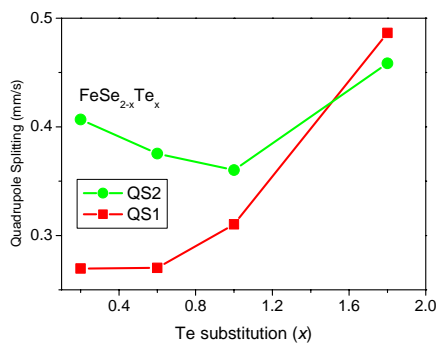
Fig.5. Mössbauer Spectra at 300K of Fe(Se<sub>2-x</sub>Te<sub>x</sub>) with x= 0.2,0.6,1.0,1.4&1.8



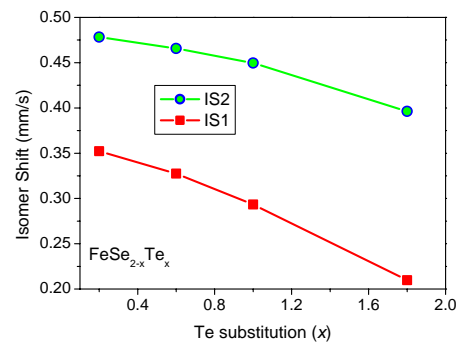
(i)



(ii)

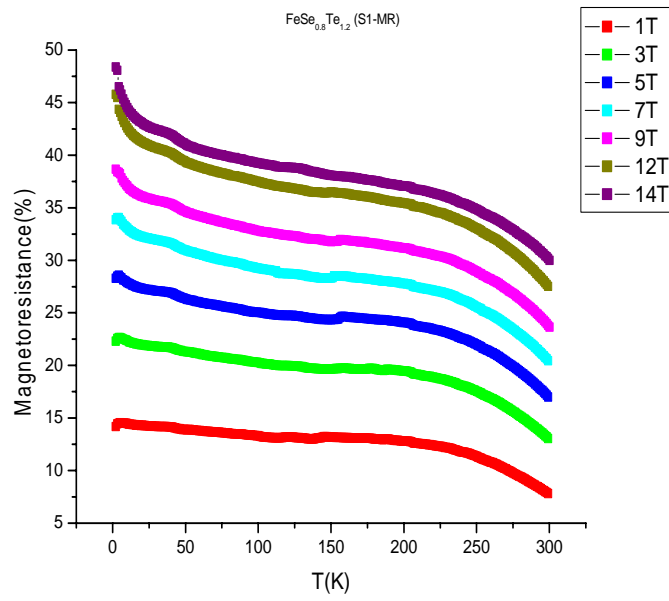
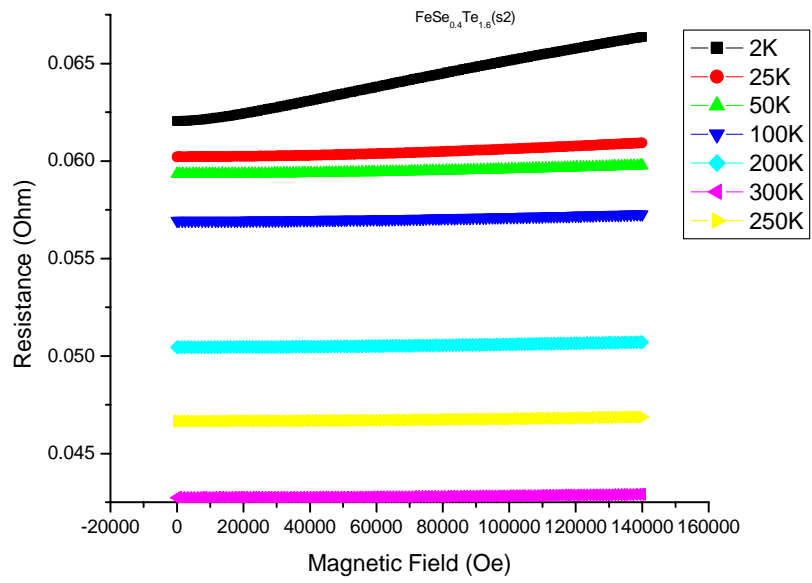


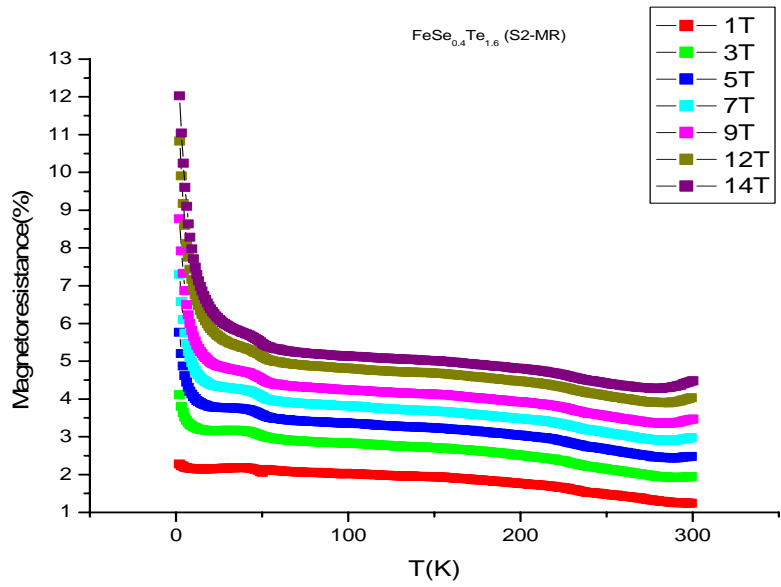
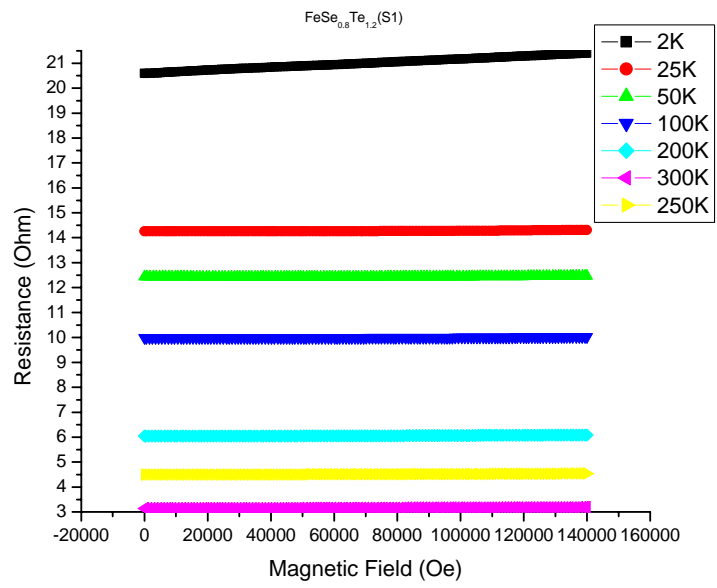
(iii)



(iv)

Fig.7. Variation in Mössbauer parameters at 300K for  $\text{FeSe}_{2-x}\text{Te}_x$  with Te





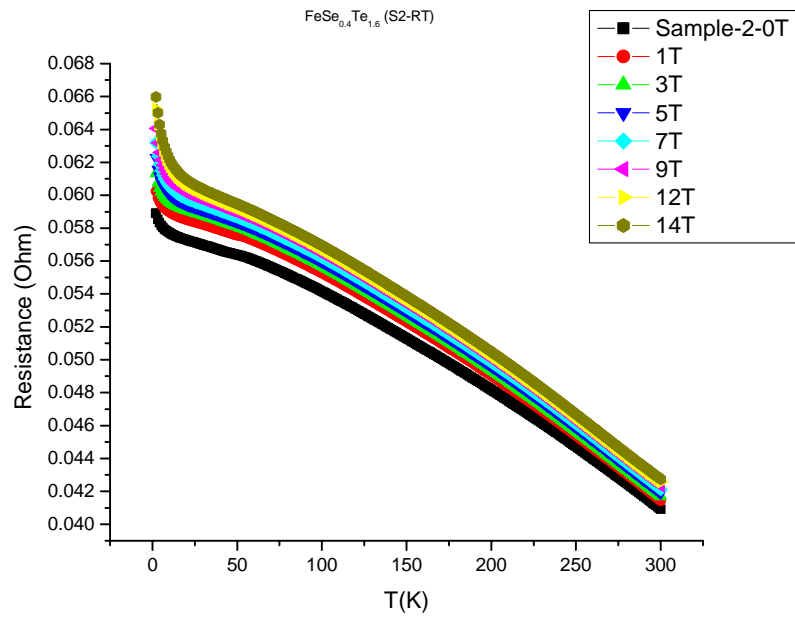


Fig.8. Variation of resistance with magnetic field at different temperature

Table I

Lattice parameters (a, b, c) and unit cell volume (V) for all five compositions

Specimen	a(Å)	b(Å)	c(Å)	c/a	c/b	V( $10^{-30}\text{m}^3$ )
FeSe <sub>2</sub>	5.825	4.827	3.597	0.618	0.745	101.138
	5.822*	4.838*	3.609*	0.620*	0.746*	101.654*
FeSe <sub>1.6</sub> Te <sub>0.4</sub>	5.625	4.982	3.629	0.645	0.728	103.698
FeSe <sub>1.2</sub> Te <sub>0.8</sub>	5.540	5.232	3.682	0.665	0.704	106.724
FeSe <sub>1.0</sub> Te <sub>1.0</sub>	5.486	5.438	3.740	0.682	0.688	111.575
FeSe <sub>0.8</sub> Te <sub>1.2</sub>	5.362	5.880	3.812	0.711	0.648	120.187
FeSe <sub>0.4</sub> Te <sub>1.6</sub>	5.328	5.992	3.818	0.717	0.637	121.891
FeTe <sub>2</sub>	5.275	6.269	3.872	0.734	0.618	128.043
	5.267*	6.267*	3.869*	0.735*	0.619*	127.707*

Table II

Mössbauer parameters at 300K for FeSe<sub>2-x</sub>Te<sub>x</sub> system for isomer shift  $\delta$  is given with respect to  $\alpha$ -Fe

Specimen Name	IS (mm/s)		QS(mm/s)		LW(mm/s)		Area Ratio		$\chi^2$ -
	Site A	Site B	Site A	Site B	Site A	Site B	Site A	Site B	
FeSe <sub>1.8</sub> Te <sub>0.2</sub>	0.35229 ( $\pm 0.0171$ )	0.4782 ( $\pm 0.0000$ )	0.2696 ( $\pm 0.0365$ )	0.4067 ( $\pm 0.0787$ )	0.4328 ( $\pm 0.0000$ )	0.2534 ( $\pm 0.0000$ )	0.8407	0.1592	0.8822
FeSe <sub>1.4</sub> Te <sub>0.6</sub>	0.3275 ( $\pm 0.0000$ )	0.4657 ( $\pm 0.0000$ )	0.2902 ( $\pm 0.0000$ )	0.3783 ( $\pm 0.0175$ )	0.3835 ( $\pm 0.0000$ )	0.2673 ( $\pm 0.0000$ )	0.7075	0.2924	1.067
FeSe <sub>1.0</sub> Te <sub>1.0</sub>	0.2934 ( $\pm 0.0191$ )	0.4495 ( $\pm 0.0000$ )	0.3102 ( $\pm 0.0000$ )	0.3601 ( $\pm 0.0162$ )	0.3300 ( $\pm 0.0000$ )	0.2826 ( $\pm 0.0340$ )	0.5035	0.4964	0.9983
FeSe <sub>0.2</sub> Te <sub>1.8</sub>	0.2096 ( $\pm 0.0150$ )	0.3962 ( $\pm 0.0042$ )	0.4864 ( $\pm 0.0206$ )	0.4584 ( $\pm 0.0069$ )	0.2566 ( $\pm 0.0000$ )	0.3324 ( $\pm 0.0138$ )	0.1870	0.8129	0.8608